RADIAL EVOLUTION OF CROSS HELICITY AT LOW AND HIGH LATITUDES IN THE SOLAR WIND

B. Breech[1], W. H. Matthaeus[1], J. Minnie[2], S. Oughton[3], S. Parhi[1], J. W. Bieber[1], and B. Bavassano[4]

[1]Bartol Research Institute, University of Delaware, Newark, Delaware 19716, USA
[2]School of Physics, North-West University, Potchefstroom, South Africa
[3]Department of Mathematics, University of Waikato, Hamilton, New Zealand
[4]Istituto di Fisica dello Spazio Interplanetario, Consiglio Nazionale delle Ricerche, Rome, Italy

ABSTRACT

We employ a turbulence transport theory to the radial evolution of the solar wind at both low and high latitudes. The theory includes cross helicity, magnetohydrodynamic (MHD) turbulence, and driving by shear and pickup ions. The radial decrease of cross helicity, observed in both low and high latitudes, can be accounted for by including sufficient shear driving to overcome the tendency of MHD turbulence to produce Alfvénic states. The shear driving is weaker at high latitudes leading to a slower evolution. Model results are compared with observations from Ulysses and Voyager.

1. INTRODUCTION

The evolution of solar wind turbulence is a challenging space plasma physics problem, and one that is central in understanding various features of the heliosphere including radial temperature, solar energetic particles and modulation of galactic cosmic rays. Relatively complete formalisms for turbulence transport in a weakly inhomogeneous medium have been developed using several complementary approaches [1, 2, 3]. Frequently further approximations are imposed to achieve a physically transparent model. One of those simplifications is to the case of zero cross helicity or, equivalently, equal admixtures of inward and outward Alfvénic fluctuations. This is probably well satisfied beyond a heliocentric distance of a few Astronomical Units (AU), but it is marginal from 1–3 AU, and is definitely not a reasonable simplification at distances less than 1 AU from the sun [4, 5, 6, 7, 8].

Recent work [9, 10] has focused on developing a turbulence transport model for the solar wind which allows for mixed cross helicities. In this paper, we apply the model to the solar wind at both low and high latitudes. The application of the model differs in the two regimes by reasonable changes to characteristic parameters.

2. MODEL AND PARAMETERS

Several features of MHD turbulence are relevant to understanding the evolution of solar wind fluctuations. First, the general scenario of cascade and decay of homogeneous MHD turbulence is found to proceed in much the same way as in hydrodynamics [11]. Second, MHD cascades can be strongly anisotropic. Spectral transfer is stronger in the directions perpendicular to the large-scale mean magnetic field, and is weaker in the parallel direction, leading to relatively stronger cross-field gradients of magnetic, velocity, and small-scale density fluctuations [12]. Third, for the weakly inhomogeneous solar wind flow, a generalization of WKB theory [2, 1, 13] describes the transport of "locally homogeneous" MHD turbulence. Fourth, for low plasma-frame Mach number the local turbulence can be described approximately by a nearly incompressible (NI) MHD theory [14, 15] in which the leading-order nonlinear effects are anisotropic and incompressible. These factors may be assembled into a quantitative description of turbulence transport and decay that, with some simplifications, can be applied to the solar wind in relatively tractable form [16, 17, 18, 19].

In the absence of strong large-scale velocity shear, dynamic alignment [20, 21] tends to increase the Alfvénicity, in the sense that the cross helicity $H_c = \frac{1}{2}\langle \mathbf{v} \cdot \mathbf{b} \rangle$ of the velocity $\mathbf{v}$ and magnetic field $\mathbf{b}$ fluctuations decreases more slowly than does the incompressible energy density (per unit mass) $E = \frac{1}{2}\langle |\mathbf{v}|^2 + |\mathbf{b}|^2 \rangle$. (Angle brackets denote an appropriate averaging procedure.) Quantitatively, dynamic alignment is signified by growth of the normalized cross helicity $\sigma_c = 2H_c/E = (Z_+^2 - Z_-^2)/(Z_+^2 + Z_-^2)$, with $Z_\pm^2 = \langle |\mathbf{v} \pm \mathbf{b}|^2 \rangle$. Shear driving generally supplies equal energy in "forward" (Z_+, say) and "backward" (Z_-) type fluctuations, which in linear theory are eigenmodes associated with unidirectional propagation. Hence shear driving opposes dynamic alignment, which on its own would act to increase the Alfvénicity.

Here we will compare the predictions of a four-equation

turbulence model with observations of the radial decrease of normalized cross helicity. The turbulence model includes equations for turbulence energy $Z^2 = (Z_+^2 + Z_-^2)/2$, similarity or correlation lengthscale λ, proton temperature T, and normalized cross helicity σ_c. The equations are steady-state, and employ a uniform large-scale solar wind speed U and specified radial profiles for the Alfvén speed and density. Turbulence is considered to be locally homogeneous and incompressible, following an MHD adaptation of a Kármán–Taylor phenomenology [16, 22]. The equations are,

$$\frac{\mathrm{d}Z^2}{\mathrm{d}r} = -\frac{Z^2}{r} + \frac{C_{\rm sh} - M\sigma_D}{r} Z^2 + \frac{\dot{E}_{PI}}{U} - \frac{\alpha}{\lambda U} f^+(\sigma_c) Z^3, \quad (1)$$

$$\frac{\mathrm{d}\lambda}{\mathrm{d}r} = \frac{M\sigma_D - \hat{C}_{\rm sh}}{r}\lambda - \frac{\beta}{\alpha}\lambda\frac{\dot{E}_{PI}}{UZ^2} + \frac{\beta}{U} f^+(\sigma_c) Z, \quad (2)$$

$$\frac{\mathrm{d}\sigma_c}{\mathrm{d}r} = \alpha f'(\sigma_c)\frac{Z}{U\lambda} - \left[\frac{C_{\rm sh} - M\sigma_D}{r} + \frac{\dot{E}_{PI}}{UZ^2}\right]\sigma_c, \quad (3)$$

$$\frac{\mathrm{d}T}{\mathrm{d}r} = -\frac{4}{3}\frac{T}{r} + \frac{1}{3}\frac{m_p}{k_B}\frac{\alpha}{U} f^+(\sigma_c)\frac{Z^3}{\lambda}. \quad (4)$$

Three functions of the cross helicity were introduced to simplify the notation. They are,

$$f^{\pm}(\sigma_c) = \frac{(1-\sigma_c^2)^{1/2}}{2}\left[(1+\sigma_c)^{1/2} \pm (1-\sigma_c)^{1/2}\right], \quad (5)$$

and

$$f'(\sigma_c) = \left[\sigma_c f^+(\sigma_c) - f^-(\sigma_c)\right] \approx \frac{\sigma_c - \sigma_c^3}{2}. \quad (6)$$

The model depends upon various parameters, including Kármán–Taylor constants, chosen here as $\alpha = 2\beta = 0.8$, a mixing constant $M = 1/2$, $\sigma_D = \langle|\mathbf{v}|^2 - |\mathbf{b}|^2\rangle/2E = -1/3$ (assumed constant). See, e.g., [22].

Turbulence is driven by two effects. First, large-scale shear instability supplies turbulence energy. This is represented by constants $C_{\rm sh}$ and $\hat{C}_{\rm sh}$ that control the shear strength. (Here we take $\hat{C}_{\rm sh} = 0$ appropriate to driving at roughly the correlation scale.) Second, scattering of ionized interstellar neutrals (pickup ions) supplies energy through wave-particle interactions, represented here by the term $\dot{E}_{PI}$. The form of pickup ion driving we employ is the same as in [18] (for an updated form, see [19]). Pickup ion driving of turbulence is important beyond 10 AU and is not the focus of the present study.

The main focus of the present paper is the radial evolution of normalized cross helicity σ_c. Using the approximation given in Eq. (6), we examine threshold estimates of the interplanetary conditions needed to account for the typical observation that σ_c decreases with increasing heliocentric distance [23, 7]. Rearranging Eq. (3) we find

$$\frac{\mathrm{d}\sigma_c}{\mathrm{d}r} \approx \left[\frac{\alpha}{2}(1-\sigma_c^2)\frac{Z}{U\lambda} - \frac{C_{\rm sh} - M\sigma_D}{r} - \frac{\dot{E}_{PI}}{UZ^2}\right]\sigma_c. \quad (7)$$

Thus, σ_c decays towards zero provided the square-bracketed term is negative. Consequently the observations require, approximately, that

$$C_{\rm sh} - M\sigma_D + \frac{r\dot{E}_{PI}}{UZ^2} > \alpha\frac{(1-\sigma_c^2)}{2}\frac{rZ}{U\lambda}. \quad (8)$$

Note that usually $M\sigma_D \approx -1/6 << C_{\rm sh}$ [3]. In the middle heliosphere, say $0.3\,\mathrm{AU} < r < 10\,\mathrm{AU}$, pickup ion effects are not important, and Eq. (8) simplifies to

$$C_{\rm sh} > \alpha\frac{(1-\sigma_c^2)}{2}\frac{rZ}{U\lambda}. \quad (9)$$

The fraction $rZ/\lambda U$, interpretable as the ratio of the expansion and nonlinear timescales, is often of order unity in the solar wind. We see that there exists a threshold in shear strength above which σ_c decreases with radius.

The shear constant is estimated using $\Delta U/\Delta r = C_{\rm sh}U/r$ [2, 16]. The strength of shear driving of turbulence is expected to differ in low latitude and high latitude solar wind. In particular, a lower value of $C_{\rm sh}$ is expected in the high latitude fast wind, due to the absence of large stream interfaces. We find [10] that $C_{\rm sh} \sim 1.5$ for the low latitudes and $C_{\rm sh} \approx 1/2$ for the high latitudes works well to account for the solar wind turbulence evolution. Note that these values of $C_{\rm sh}$ are high enough that the condition given in equation (9) should be satisfied for high values of σ_c thought to be apparent in the innermost heliosphere (say, $r = 0.3$ AU). We can thus expect a decrease in the cross helicity in the innermost part of the heliosphere.

3. LOW LATITUDE RESULTS

We used the model to compute solutions at both low and high latitudes and compare the results to observations. Figure 1 shows a sample solution in the ecliptic plane, where the cross helicity is observed to decrease with heliocentric distance [5, 6, 7, 8].

Note that we have used parameters (see caption) in the transport model that are comparable to values employed by [18] The model results are compared to observational points adapted from [7], as well as two 1 AU data points from the OMNI data set. Evidently the transport theory accounts reasonably well for the observed decrease of σ_c vs. r, providing further support for the suggestion [24] that Alfvénicity is reduced by turbulence driven by shear in solar wind stream structure. Note, however, that the adapted data points are not properly sorted, e.g., by wind speed. Consequently a more careful comparision with observations is needed. The present results also motivate further examination of latitude effects on solar wind cross helicity [25, 23, 26].

4. HIGH LATITUDE RESULTS

Figure 2 shows solutions computed by the model at high latitude. The solutions are compared with hourly σ_c val-

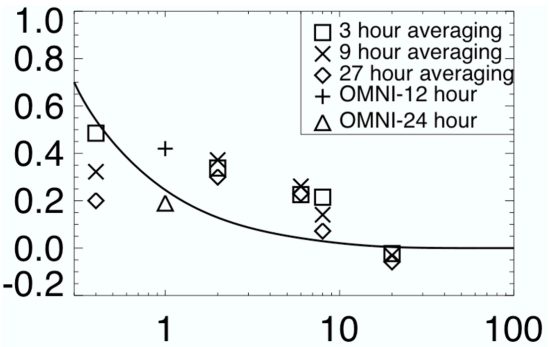

Figure 1. Radial evolution of normalized cross helicity σ_c at low latitudes, near the ecliptic plane. Observational values extracted from Helios and Voyager data, are suggested by the symbols, which are adapted from [7] (courtesy of D. A. Roberts). Additionally, two data points from the OMNI data set are also included. The parameters used for the model solution are appropriate to low latitudes; shear strength $C_{\rm sh} = 1.5$, mixing parameter $M\sigma_D = -1/6$, a standard form of the pickup driving term (see Smith et al.*2001), and constants $\alpha = 2\beta = 0.8$, with boundary data at 0.3 AU specified as $Z^2 = 2200$ km^2/sec^2, $\lambda = 0.01$ AU and $\sigma_c = 0.7$*

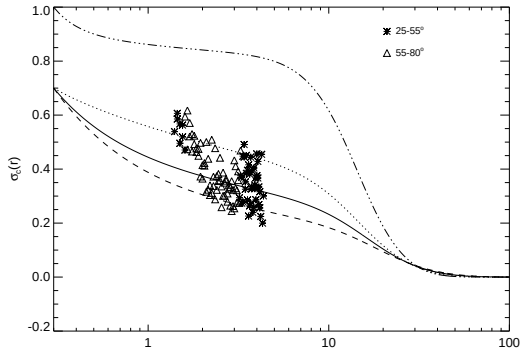

Figure 2. Radial evolution of normalized cross helicity σ_c at high latitudes. Observational points from Ulysses data in two latitude bands (see legend). Three solutions for $\sigma_c(r)$ from the transport equations are shown, for a fixed latitude of 75° and varying values of turbulence level and correlation scale at the boundary: Dotted curve*: $Z^2 = 10000\,km^2\,s^{-2}$ and $\lambda = 0.02\,AU$;* Solid curve*: $Z^2 = 6000\,km^2\,s^{-2}$ and $\lambda = 0.04\,AU$;* Dashed curve $Z^2 = 4500\,km^2\,s^{-2}$ *and $\lambda = 0.07\,AU$. All other parameters are fixed. Appropriate to high latitudes [27], we take $U = 774$ km/s and an Alfvén speed at 1 AU of 51 km/s. The driving parameters are $C_{\rm sh} = 0.5$ and $M\sigma_D = -1/6$, with a standard pickup driving term [18].Note that lower Z^2 and higher λ at the inner boundary produces more rapid radial decrease of σ_c.*

ues from *Bavassano et al.* (2000a,b), computed from Ulysses data. There is no attempt to examine systematic variation with latitude—we plot values of σ_c for two ranges of latitude (moderately high 25–55° and very high 55–80°). All points have $\theta > 25^\circ$.

As there is considerable spread in the data, we have plotted three solutions for $\sigma_c(r)$ from the theory. The three solutions differ in the imposed inner boundary values for the turbulence amplitude Z^2 and the correlation scale λ. Relative to low latitude solutions (figure 1), these solutions use lower $C_{\rm sh}$, higher solar wind speed, and lower density [27]. The three solutions show that a moderate (and realistic) variation of inner boundary values produces theoretical curves that vary in a way that is comparable to the scatter in the Ulysses data. A fourth solution is also shown, with identical parameters, except that $\sigma_c = 1.0$ (maximal value) at the inner boundary, and $C_{\rm sh}$ was reduced. This solution represents a pure Alfvénic stream, with higher σ_c, as might be inferred from some studies (e.g., *Goldstein et al.*, 1995)).

We recall the suggestion [*Bavassano et al.*, 2000a,b] that the cross helicity saturates, i.e., approaches a terminal nonzero value in the high latitude wind. This tendency is apparent in Figure 2: Between 1.5 AU and 3 AU there is a downward trend. However there is no clear downward trend for data beyond 3 AU. Note the substantial spread in observed values of $\sigma_c(r)$ near any r.

5. CONCLUSION

We have presented a turbulence transport model that has been extended to include non-zero cross helicities [9, 10]. The model accounts reasonably well for observations in both the high and low latitude solar wind. The parameters characterizing the model differ in the two regimes in reasonable ways, including lower shear in the high latitude wind. It is beyond the scope of the current paper to fully explore the implications of the model solutions at different latitudes. Such a study will be presented in the future.

REFERENCES

1. Marsch, E. and Tu, C.-Y. Dynamics of correlation functions with Elsässer variables for inhomogeneous MHD turbulence. *J. Plasma Phys.*, **41**:479, 1989.

2. Zhou, Y. and Matthaeus, W. H. Transport and turbulence modeling of solar wind fluctuations. *J. Geophys. Res.*, **95**:10 291, 1990.

3. Matthaeus, W. H., Oughton, S., Pontius, D., and Zhou, Y. Evolution of energy containing turbulent eddies in the solar wind. *J. Geophys. Res.*, **99**:19 267–19 287, 1994.

4. Belcher, J. W. and Davis Jr., L. Large-amplitude Alfvén waves in the interplanetary medium, 2. *J. Geophys. Res.*, **76**:3534–3563, 1971.

5. Bavassano, B., Dobrowolny, M., Mariani, F., and Ness, N. F. Radial evolution of power spectra of interplanetary Alfvénic turbulence. *J. Geophys. Res.*, **87**:3617, 1982.

6. Bavassano, B., Dobrowolny, M., Fanfoni, G., Mariani, F., and Ness, N. F. Statistical properties of MHD fluctuations associated with high-speed streams from Helios-2 observations. *Solar Phys.*, **78**:373, 1982.

7. Roberts, D. A., Goldstein, M. L., Klein, L. W., and Matthaeus, W. H. Origin and evolution of fluctuations in the solar wind: Helios observations and Helios-Voyager comparisons. *J. Geophys. Res.*, **92**:12 023–12 035, 1987.

8. Tu, C.-Y., Roberts, D. A., and Goldstein, M. L. Spectral evolution and cascade of solar wind Alfvénic turbulence. *J. Geophys. Res.*, **94**:13 575, 1989b.

9. Matthaeus, W. H., Minnie, J., Breech, B., Parhi, S., Bieber, J. W., and Oughton, S. Transport of cross helicity and the radial evolution of Alfvénicity in the solar wind. *Geophys. Rev. Lett.*, **31**:L12803, doi:10.1029/2004GL019645, 2004.

10. Breech, B., Matthaeus, W. H., Minnie, J., Oughton, S., Parhi, S., and Bieber, J. W. Radial evolution of cross helicity in high-latitude solar wind. *Geophys. Rev. Lett.*, **32**:L06103,doi:10.1029/2004GL022321, 2005.

11. Hossain, M., Gray, P. C., Pontius Jr., D. H., Matthaeus, W. H., and Oughton, S. Phenomenology for the decay of energy-containing eddies in homogeneous MHD turbulence. *Phys. Fluids*, **7**:2886–2904, 1995.

12. Shebalin, J. V., Matthaeus, W. H., and Montgomery, D. Anisotropy in MHD turbulence due to a mean magnetic field. *J. Plasma Phys.*, **29**:525–547, 1983.

13. Matthaeus, W. H., Zhou, Y., Zank, G. P., and Oughton, S. Transport theory and the WKB approximation for interplanetary MHD fluctuations. *J. Geophys. Res.*, **99**:23 421–23 430, 1994.

14. Zank, G. P. and Matthaeus, W. H. Waves and turbulence in the solar wind. *J. Geophys. Res.*, **97**:17 189–17 194, 1992.

15. Zank, G. P. and Matthaeus, W. H. Nearly incompressible fluids. II: Magnetohydrodynamics, turbulence, and waves. *Phys. Fluids A*, **5**:257–273, 1993.

16. Zank, G. P., Matthaeus, W. H., and Smith, C. W. Evolution of turbulent magnetic fluctuation power with heliocentric distance. *J. Geophys. Res.*, **101**:17 093, 1996.

17. Matthaeus, W. H., Zank, G. P., Smith, C. W., and Oughton, S. Turbulence, spatial transport, and heating of the solar wind. *Phys. Rev. Lett.*, **82**:3444–3447, 1999.

18. Smith, C. W., Matthaeus, W. H., Zank, G. P., Ness, N. F., Oughton, S., and Richardson, J. D. Heating of the low-latitude solar wind by dissipation of turbulent magnetic fluctuations. *J. Geophys. Res.*, **106**:8253–8272, 2001.

19. Isenberg, P. A., Smith, C. W., and Matthaeus, W. H. Turbulent heating of the distant solar wind by interstellar pickup protons. *Astrophys. J.*, **592**:564–573, 2003.

20. Dobrowolny, M., Mangeney, A., and Veltri, P. Fully developed anisotropic hydromagnetic turbulence in interplanetary space. *Phys. Rev. Lett.*, **45**:144–147, 1980.

21. Pouquet, A., Meneguzzi, M., and Frisch, U. Growth of correlations in magnetohydrodynamic turbulence. *Phys. Rev. A*, **33**:4266–4275, 1986.

22. Matthaeus, W. H., Zank, G. P., and Oughton, S. Phenomenology of hydromagnetic turbulence in a uniformly expanding medium. *J. Plasma Phys.*, **56**:659–675, 1996.

23. Bavassano, B., Pietropaolo, E., and Bruno, R. Alfvénic turbulence in the polar wind: A statistical study on cross helicity and residual energy variations. *J. Geophys. Res.*, **105**:12 697–12 704, 2000.

24. Roberts, D. A., Goldstein, M. L., Matthaeus, W. H., and Ghosh, S. Velocity shear generation of solar wind turbulence. *J. Geophys. Res.*, **97**:17 115, 1992.

25. Goldstein, M. L., Roberts, D. A., and Ghosh, S. Numerical simulations of large-scale solar wind fluctuations observed by Ulysses at high heliographic latitudes. *Geophys. Rev. Lett.*, **22**:3413, 1995.

26. Bavassano, B., Pietropaolo, E., and Bruno, R. On the evolution of outward and inward Alfvénic fluctuations in the polar wind. *J. Geophys. Res.*, **105**:15 959–15 964, 2000.

27. McComas, D. J., Barraclough, L., Funsten, H. O., Gosling, J. T., Santiago-Muñoz, E., Skoug, R. M., Goldstein, B. E., Neugebauer, M., Riley, P., and Balogh, A. Solar wind observations over Ulysses' first full polar orbit. *J. Geophys. Res.*, **105**:10 419–10 434, 2000.

28. Goldstein, B. E., Smith, E. J., Balogh, A., Horbury, T. S., Goldstein, M. L., and Roberts, D. A. Properties of magnetohydrodynamic turbulence in the solar wind as observed by Ulysses at high heliographic latitudes. *Geophys. Rev. Lett.*, **22**:3393, 1995.